CONFERENCE PRE-PRINT

DRIFT-KINETIC AND FULLY KINETIC SIMULATIONS OF PLASMA WAVES BASED ON A GEOMETRIC PARTICLE-IN-CELL DISCRETIZATION OF THE VLASOV-MAXWELL SYSTEM

Guo Meng
Max Planck Institute for Plasma Physics
Garching, Germany
Email: guo.meng@ipp.mpg.de

Katharina Kormann
Department of Mathematics, Ruhr University Bochum
Bochum, Germany

Emil Poulsen
Max Planck Institute for Plasma Physics
Garching, Germany

Eric Sonnendrücker
Max Planck Institute for Plasma Physics
Garching, Germany
School of Computation Information and Technology, Technical University of Munich
Garching, Germany

Abstract

In this work, we extend the geometric Particle in Cell framework on dual grids to a gauge-free drift-kinetic Vlasov–Maxwell model and its coupling with the fully kinetic model. We derive a discrete action principle on dual grids for our drift-kinetic model, such that the dynamical system involves only the electric and magnetic fields and not the potentials as most drift-kinetic and gyrokinetic models do. This yields a macroscopic Maxwell equation including polarization and magnetization terms that can be coupled straightforwardly with a fully kinetic model.

1. INTRODUCTION

Most current gyrokinetic codes in the magnetically confined fusion community are based on the traditional scalar and vector potential formulation, typically considering only the parallel component of the vector potential. These studies are generally limited to specific branches or a few types of instabilities, such as drift-wave turbulence or Alfvénic modes. In contrast, we have developed a gauge-free drift-kinetic Vlasov–Maxwell model coupled with a fully kinetic description of ions [1], extending the geometric Particle-In-Cell (PIC) framework on dual grids [2]. The approach relies on a discrete action principle using only the electric and magnetic fields, avoiding the use of potentials. The resulting macroscopic Maxwell equations incorporate polarization and magnetization terms, enabling seamless coupling with a fully kinetic model for treating energetic particles and edge physics. The hybrid model highlights the ability to resolve ion-cyclotron frequency ranges [1]. Notice however that we don't add any approximation beyond the gyrokinetic particle Lagrangian. This means that light waves and compressional Alfvén waves are still present in our drift-kinetic models. Addressing Darwin like and quasi-neutrality assumptions to remove these high frequency waves will be the purpose of future work.

Plasma physics models often exhibit a Hamiltonian structure with conserved invariants such as the Hamiltonian, Gauss's law, and $\nabla \cdot \boldsymbol{B} = 0$ [3, 4]. Structure-preserving numerical methods aim to maintain these invariants for stable numerical solutions. The geometric approach discretizes the Hamiltonian structure rather than the partial differential equations, ensuring conservation of appropriately discretized invariants [5].

Earlier studies introduced hybrid kinetic models using the E&B formulation directly [6, 7]. As noted in [6, 8], the compressional Alfvén mode imposes the most stringent constraint on the time step when $k_\theta \rho_i \sim 1$, advanced numerical methods such as the implicit methods [9] are necessary for overcoming this constraint. The gyrokinetic E&B models developed in previous works for low-frequency electromagnetic fluctuations [10], kinetic Alfvén waves in tokamak plasmas [8] and hybrid model [6, 7] differ from our approach in both the formulations and the focus on geometric numerical methods for discretizing the equations. A key feature of our approach is that we derive both the field and particle equations of motion from a Lagrangian coupling drift-kinetic electrons with fully kinetic ions at the continuous level, ensuring numerical consistency and structure preserving in the discretized space. This contrasts with the treatment that separately discretizes the physical field and particle equations, for which maintaining the same conservation laws as in the continuous Lagrangian can be challenging.

Beginning with the gyrokinetic Lagrangian of Burby and Brizard [11] in the Zero Larmor Radius limit, we develop a Lagrangian that couples drift-kinetic electrons with fully kinetic ions at the continuous level. We then propose a discretized version of the Lagrangian based on the Mimetic Finite Difference framework on dual grids [2] and the PIC method. From this discretized formulation, we derive the equations of motion for the PIC markers, as well as the discrete generalized Maxwell equations, which include polarization and magnetization terms arising from the drift-kinetic particles. The hybrid kinetic model integrates both kinetic and drift-kinetic contributions, providing a unified framework applicable to edge plasma physics in magnetic confinement fusion devices.

2. A GAUGE-FREE DRIFT-KINETIC MODEL

The equations of motion

$$\frac{\mathrm{d}\boldsymbol{X}}{\mathrm{d}t} = V_\shortparallel \frac{\boldsymbol{B}^*}{B^*_\shortparallel} + \frac{1}{B^*_\shortparallel}\left(\boldsymbol{E}\times\boldsymbol{b}_{\text{ext}} - \frac{\mu}{q_e}\nabla B_{\shortparallel,\text{tot}}\times\boldsymbol{b}_{\text{ext}}\right) = \boldsymbol{v}_{gc}, \tag{1}$$

$$\frac{\mathrm{d}V_\shortparallel}{\mathrm{d}t} = \frac{q}{m}\frac{\boldsymbol{B}^*}{B^*_\shortparallel}\cdot\left(\boldsymbol{E} - \frac{\mu}{q}\nabla B_{\shortparallel,\text{tot}}\right) = a_{gc}. \tag{2}$$

The a macroscopic Maxwell system including polarization and magnetization effects coming from the drift-kinetic particles (in strong form)

$$\frac{\partial\boldsymbol{D}}{\partial t} - \nabla\times\boldsymbol{H} = -\boldsymbol{J}_{gc}, \tag{3}$$

$$\frac{\partial\boldsymbol{B}}{\partial t} + \nabla\times\boldsymbol{E} = 0, \tag{4}$$

$$\nabla\cdot\boldsymbol{D} = \rho_{gc}, \tag{5}$$

$$\nabla\cdot\boldsymbol{B} = 0. \tag{6}$$

Equation (5) is guaranteed to hold at all times, as long as it is satisfied at the initial time and Eq. (6) is preserved by the numerical discretization. The displacement field $\boldsymbol{D}$ and the magnetic field intensity $\boldsymbol{H}$ by

$$\boldsymbol{D} = \epsilon_0\boldsymbol{E} + \mathbf{P}, \tag{7}$$

$$\boldsymbol{H} = \frac{1}{\mu_0}(\boldsymbol{B}_{\text{ext}} + \boldsymbol{B}) - \mathbf{M} \tag{8}$$

as well as the polarization $\mathbf{P}$ and the magnetization $\mathbf{M}$

$$\mathbf{P}(t,\boldsymbol{x}) = \frac{m}{|\boldsymbol{B}_{\text{ext}}|^2}\int(\boldsymbol{E}_\perp + v_\shortparallel\boldsymbol{b}_{\text{ext}}\times\boldsymbol{B}) f B^*_\shortparallel \,\mathrm{d}v_\shortparallel\,\mathrm{d}\mu. \tag{9}$$

$$\mathbf{M}(t,\boldsymbol{x}) = \int\left[-\mu\boldsymbol{b}_{\text{ext}} - \frac{\mu\boldsymbol{B}_\perp}{|\boldsymbol{B}_{\text{ext}}|} + \frac{m}{|\boldsymbol{B}_{\text{ext}}|^2}({v_\shortparallel}^2\boldsymbol{B}_\perp + v_\shortparallel\boldsymbol{E}\times\boldsymbol{b}_{\text{ext}})\right] f B^*_\shortparallel\,\mathrm{d}v_\shortparallel\,\mathrm{d}\mu. \tag{10}$$

The guiding center current

$$\boldsymbol{J}_{gc} = q\int\boldsymbol{v}_{gc} f B^*_\shortparallel\,\mathrm{d}v_\shortparallel\,\mathrm{d}\mu. \tag{11}$$

3. DISCRETIZATION WITH MIMETIC FINITE DIFFERENCES

The study employs a Mimetic Finite Difference (MFD) discretization scheme on dual grids [2]. Scalar and vector potentials, electromagnetic fields, and current densities are discretized separately on primal and dual grids. Discrete gradient, curl, and divergence operators are constructed using Kronecker products, ensuring exact compatibility with Maxwell's equations.

The key idea is that each physical quantity carries a distinct meaning, which naturally determines its discrete representation. Potentials are evaluated at points; the action of a force is represented by its circulation along a path; currents correspond to fluxes of current density through surfaces; and charges are obtained from volume integrals of charge density. The MFD framework captures these distinctions by assigning different types of integrals to different unknowns: potentials are approximated by point values (as in standard finite differences), the electric field $\boldsymbol{E}$ by line integrals along mesh edges, the current density $\boldsymbol{J}$ and magnetic field $\boldsymbol{B}$ by fluxes through mesh faces, and the charge density ρ by cell integrals.

Figure 1a shows the corresponding degrees of freedom. On the left, the vertices of the grid are used to discretize the potentials, then the edges of the mesh in each direction will be used for the three components of for example $\boldsymbol{E}$, the fluxes through the faces orthogonal to each direction, will be used to discretize the three components of $\boldsymbol{B}$ and densities will be discretized as integrals over each cell of the mesh.

On a Cartesian grid a cell on the dual grid exactly matches a vertex on the primal grid and an edge on the primal grid exactly matches a face on the dual grid, and vice-versa, as shown in Fig. 1b. $\boldsymbol{E}$ and $\boldsymbol{B}$ are primary geometric quantities defined on the primal grid, whereas $\boldsymbol{D}$, $\boldsymbol{H}$, and $\boldsymbol{J}$ are response quantities naturally associated with the dual grid. This separation ensures both geometric and physical consistency of Maxwell's equations at the discrete level.

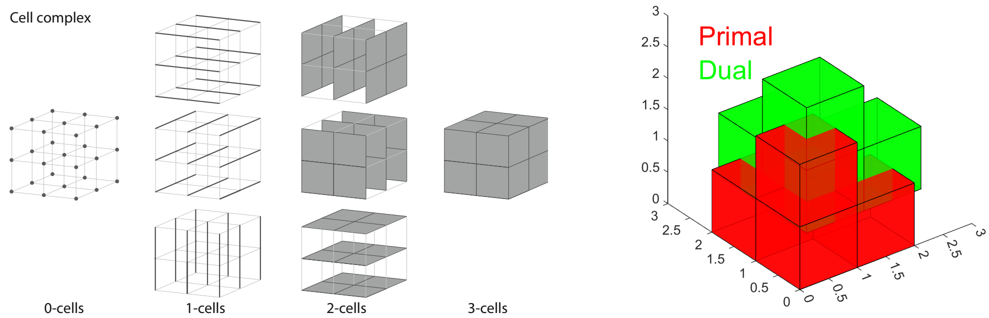

(a) Discrete unknowns on a Cartesian grid.

(b) Primal and dual grids.

FIG. 1. Degrees of freedom on the Cartesian grid (left) and the corresponding primal-dual relationships (right).

4. LOW-STORAGE RUNGE–KUTTA SCHEME FOR TIME DISCRETIZATION

A low-storage Runge-Kutta scheme is used for time discretization, optimizing memory usage in large-scale PIC simulations. We use the Williamson (2N) methods [12], which are low-storage Runge–Kutta (LSRK) schemes for solving ordinary differential equations of the form

$$u' = F(u(t)), \quad u(0) = u_0,$$

using an s-stage approach with minimum memory requirements of only one additional copy. Williamson's method is defined as follows:

$$\begin{aligned}
&S_1 := u^n \\
&\text{for } i = 1 : s \text{ do} \\
&\quad S_2 := A_i S_2 + \Delta t F(S_1) \\
&\quad S_1 := S_1 + B_i S_2 \\
&\text{end} \\
&u^{n+1} = S_1
\end{aligned} \tag{12}$$

The scheme ensures conservation of total energy, including kinetic and electromagnetic field contributions. Verification tests confirm the accuracy and stability of the numerical method.

5. SIMULATION RESULTS

5.1. Verification of drift-kinetic electrons

The dispersion relation of the drift-kinetic model is derived, demonstrating consistency with theoretical expectations. The numerical experiments validate the models by analyzing wave dispersion relations in a uniform plasma with a background magnetic field. To verify the drift-kinetic model, we first test a one-species simulation with only electrons with $v_{th,e} = c$. When $k_\perp = 0$, there are three eigenmodes. When $D_{zz} = 0$, E_z can be non-zero. It is the Langmuir wave, electrostatic perturbation is parallel to $\boldsymbol{B}_{\text{ext}}$ and parallel propagating. We initialized a density perturbation with $\rho = 1 + 0.04\cos(k_z z)$. The perturbation is electrostatic ($\boldsymbol{B} \ll \boldsymbol{E}$) and parallel to $\boldsymbol{B}_{\text{ext}}$. As shown in Fig. 2a with $k_z = 0.4$, the damping of E_z is observed, and the results are in good agreement with the analytical solution. We also fit the numerical results to determine the frequency and damping rate of the mode for varying k_z as shown by the dots in Fig. 2b. Finally, we show Fig. 2c the wave spectrum. The analytical results are displayed as lines. We observe two branches of electromagnetic waves propagating along the magnetic field.

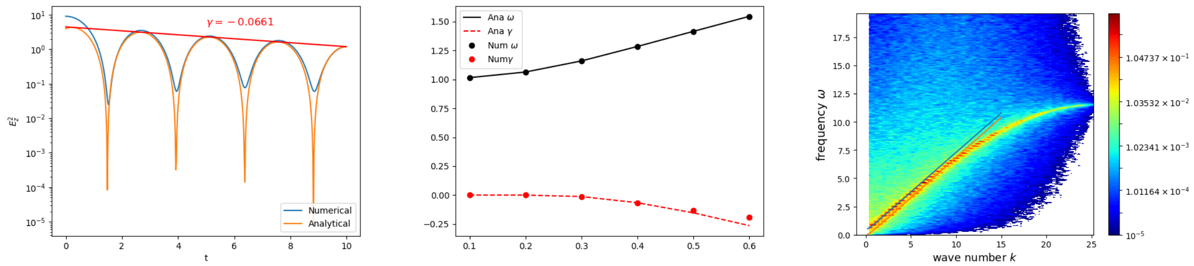

(a) Electrostatic perturbation. (b) Scan in k_z. (c) Wave spectrum

FIG. 2. Simulations with only drift-kinetic electrons

5.2. Benchmark of Fully Kinetic, Hybrid, and Drift-Kinetic Two-Species Models

To compare three modeling approaches—fully kinetic (FK) for both electrons and ions, drift-kinetic electrons with fully kinetic ions (Hybrid), and drift-kinetic (DK) for both species—we consider a two-species plasma with reduced mass ratio $m_i/m_e = 10$ and $q_i = -q_e$. The initial conditions are Gaussian distributions with thermal velocities $v_{th,e} = 0.05c$ and $v_{th,i} = 0.05c/\sqrt{10}$. We use $\omega_{pe}/|\omega_{ce}| = 1$. Consider a background magnetic field $\boldsymbol{B}_{\text{ext}} = B_{\text{ext}}\,\hat{\mathbf{z}}$. The wave vector is assumed to be in the xz plane, with $k = (k_\perp, 0, k_\parallel)$. Carrying out the tedious but straight-forward analysis, we can then obtain the following linear dispersion relation for a cold and uniform plasma. The dispersion relation is written as $\overleftrightarrow{\mathrm{D}}(\boldsymbol{k},\omega)\boldsymbol{E} = (1+\boldsymbol{\chi})\boldsymbol{E} + \frac{c^2}{\omega^2}\boldsymbol{k}\times\boldsymbol{k}\times\boldsymbol{E} = 0$. For the well known cold plasma dispersion relation (CPDR):

$$\overleftrightarrow{\mathrm{D}}(\boldsymbol{k},\omega) = \begin{bmatrix} S - n^2\cos^2\theta & -iD & n^2\sin\theta\cos\theta \\ iD & S - n^2 & 0 \\ n^2\sin\theta\cos\theta & 0 & P - n^2\sin^2\theta \end{bmatrix},$$

where $n \equiv ck/\omega$, the wave vector $\boldsymbol{k} = (k\sin\theta, 0, k\cos\theta)$.

The corresponding quantities in Stix notation [13] are:

$$S = 1 - \sum_s \frac{\omega_{ps}^2}{\omega^2 - \omega_{cs}^2}, \quad D = \sum_s \frac{\omega_{cs}\omega_{ps}^2}{\omega(\omega^2 - \omega_{cs}^2)}, \quad P = 1 - \sum_s \frac{\omega_{ps}^2}{\omega^2}.$$

When there is only one type of ion in the system besides the electrons, then we can derive the dispersion relation for the drift-kinetic electron fully-kinetic ion (Hybrid) model [7] for which

$$S = 1 + \frac{\omega_{pe}^2}{\omega_{ce}^2} - \frac{\omega_{pi}^2}{\omega^2 - \omega_{ci}^2}, \quad D = -\frac{\omega_{pe}^2}{\omega\omega_{ce}} + \frac{\omega_{ci}\omega_{pi}^2}{\omega(\omega^2 - \omega_{ci}^2)}, \quad P = 1 - \frac{\omega_p^2}{\omega^2},$$

where $\omega_p^2 = \omega_{pe}^2 + \omega_{pi}^2$. For the drift-kinetic electrons, there is no resonance at the electron cyclone frequency. And for the drift-kinetic model for both electrons and ions (DK),

$$S = 1 + \sum_s \frac{\omega_{ps}^2}{\omega_{cs}^2}, \quad D = -\sum_s \frac{\omega_{ps}^2}{\omega\omega_{cs}}, \quad P = 1 - \frac{\omega_p^2}{\omega^2}.$$

In the equations for S, D and P, the cyclotron frequency is defined as $\omega_{cs} \equiv q_s B_{\text{ext}}/m_s$. Note that q_s can be either positive or negative. The dispersion relation $\overleftrightarrow{\mathbf{D}}(\boldsymbol{k}, \omega) = 0$ can be expressed as a polynomial equation, for which established methods can be used to determine all the roots numerically [14, 1].

Later a two-species simulation compared fully kinetic, hybrid, and drift-kinetic models, revealing differences in wave dispersion properties.

5.2.1. *Waves with $\boldsymbol{k}$ perpendicular to $\boldsymbol{B}_{ext}$*

We consider a quasi-one-dimensional simulation with a domain of size $[0, 64\, d_e] \times [0, d_e] \times [0, d_e]$ and a grid of $256 \times 8 \times 8$ points, where $d_e = c/\omega_{pe}$ is the electron inertial length. We use 500 particles per cell for both species, generated by the quasi-random Sobol sampler. The particle B-spline is of degree 2 in x, y, and z directions. We employ the 5-stage fourth-order LSRK method with a time step of $\Delta t = 0.05\, \omega_{pe}^{-1}$, and the total simulation time is $T = 200\, \omega_{pe}^{-1}$. Figure 3 shows the wave spectrum along the x axis of E_x, E_y, E_z (averaged over y, z) for our different models.

The dashed lines representing the analytical results in the cold plasma limitation are obtained by solving the dispersion relations for each model. As shown in Figs. 3a, 3d and 3g, the wave spectrum aligns closely with the analytical results for the X-mode, CAW-X mode, and O-mode. At higher wave numbers, the accuracy of the numerical dispersion relation compared to the analytical results can be further improved by using a higher grid resolution. The lower X-mode asymptotes to the upper hybrid resonance. When comparing the FK and Hybrid models, the upper X-mode is absent in the Hybrid model. The X-mode in the Hybrid model has a different dispersion relation and cutoff. When ω_{pe}/ω_{ce} is smaller (low density) and m_i/m_e is larger, the cutoff frequency approximates to ω_L. And the X-mode in Hybrid mode has no resonance at ω_{UH}, as the electron cyclotron wave is absent. The transition of compressional Alfvén waves (CAW) to the X-mode branch is identical in both the FK and Hybrid models. In the DK model, even fewer modes exist as shown in the Figs. 3c and 3f. The CAW does not have resonance at ω_{LH} as the ion cyclotron effect is absent. The O-mode, which has a cutoff frequency at ω_p, exists in three models as shown in Figs. 3g, 3h and 3i. The horizontal lines in the spectrum plot of the FK model corresponding to integer values are the electron Bernstein waves since $\omega_{ce} = 1$.

5.2.2. *Waves with $\boldsymbol{k}$ parallel to $\boldsymbol{B}_{ext}$*

We use a domain of size $[0, d_e] \times [0, d_e] \times [0, 64\, d_e]$ and a grid of $8 \times 8 \times 256$ points, other parameters are the same. Then we show the numerical dispersion relation along the z axis. The results in the x-direction and y-direction are identical; therefore, we omit the E_x-direction wave spectrum in this analysis.

As shown in Fig. 4, the upper R-mode is absent in the Hybrid model compared to the FK model. In Fig. 4a, CAW denotes the compressional Alfvén waves and ECW and ICW denote electron and ion cyclotron waves. In the Hybrid model, the CAW does not transit to ECW due to the absence of electron cyclotron resonance as shown in Figs. 4a and 4b. The compressional Alfvén waves (CAW) exists resonance near ω_{LH} at k perpendicular to B and at ω_{ci} at k parallel to B as shown in Figs. 3a, 3d and Fig. 4a. The CAW-ICW branch is the same in the FK and Hybrid models. In the DK model, even fewer modes exist as shown in the Fig. 4c and the CAW does not have resonance. The waves with oscillation in E_z are the same in the three models as shown in Figs. 4d, 4e and 4f. The more accurate dispersion relation for the Langmuir wave are $D_{zz} = 0$, which are damping modes and the damping rate is stronger when k larger as shown in Fig. 2b. The resonance frequency in the cold plasma limitation is at ω_p.

As shown in Figs. 3 and 4, the hybrid model captures key plasma wave phenomena absent in purely drift-kinetic, highlighting its applicability to magnetic confinement fusion research. By combining fully kinetic ions with drift-kinetic electrons, it retains essential wave features while suppressing high-frequency electron cyclotron modes. The fully kinetic model exhibited Bernstein waves, absent in the hybrid and drift-kinetic models. These simulations illustrate how different models impact wave propagation and validate the effectiveness of the hybrid approach. The proposed geometric PIC discretization further extends structure-preserving methods to hybrid kinetic models. The Hybrid model is suitable to study the ion cyclotron frequency and low-hybrid waves without modification. When applying the Hybrid model to investigate the lower X-mode, L-mode and upper CAW branches, the applicable regime should be carefully considered. The DK model is suitable for the low-frequency CAW waves.

6. CONCLUSION AND OUTLOOK

We have developed a new geometric PIC discretization for a gauge-free drift-kinetic model that can be seamlessly integrated with a fully kinetic model. The geometric PIC framework successfully bridges drift-kinetic and fully

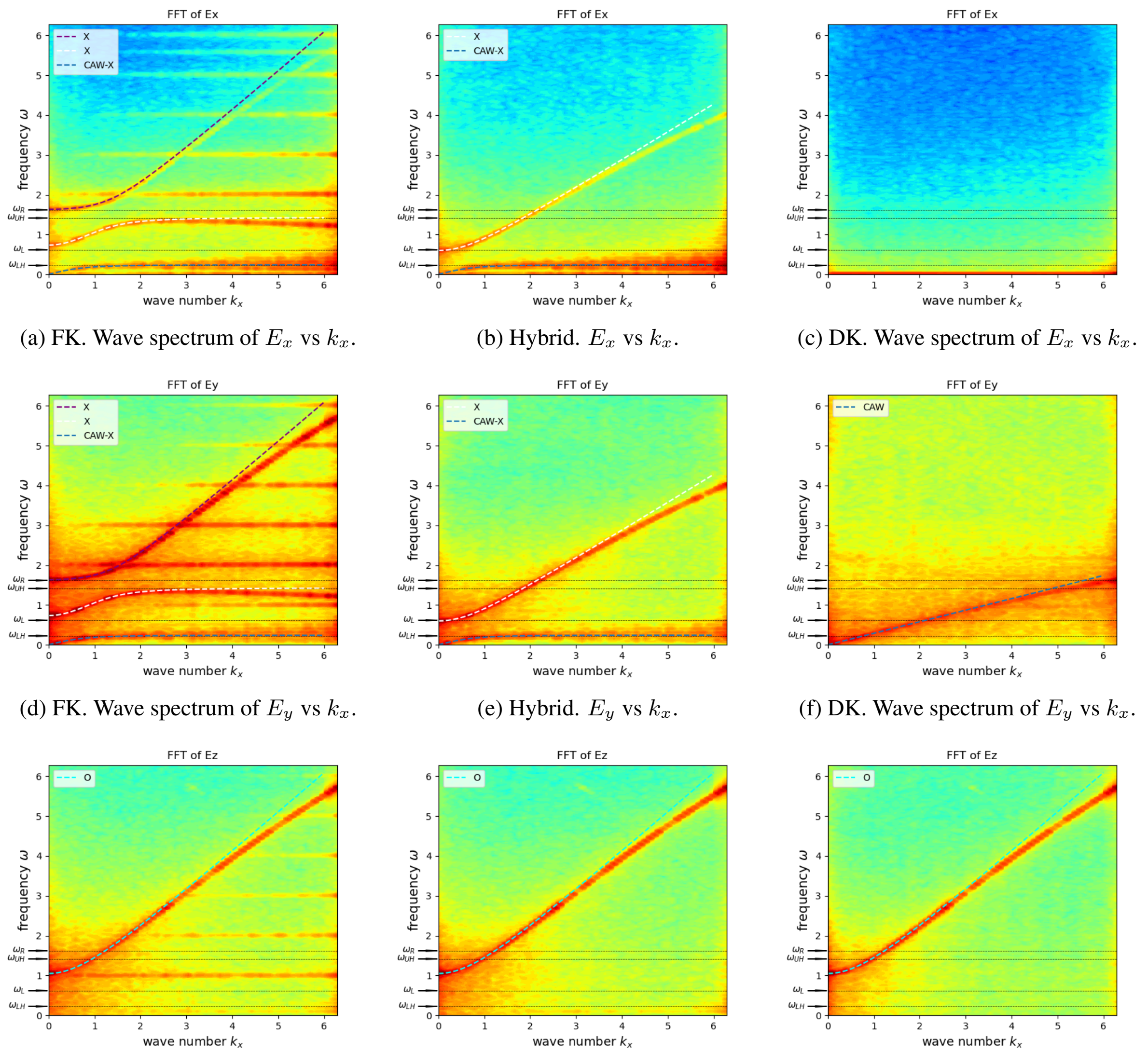

(a) FK. Wave spectrum of E_x vs k_x.

(b) Hybrid. E_x vs k_x.

(c) DK. Wave spectrum of E_x vs k_x.

(d) FK. Wave spectrum of E_y vs k_x.

(e) Hybrid. E_y vs k_x.

(f) DK. Wave spectrum of E_y vs k_x.

(g) FK. Wave spectrum of E_z vs k_x.

(h) Hybrid. E_z vs k_x.

(i) DK. Wave spectrum of E_z vs k_x.

FIG. 3. Comparison of waves with k perpendicular to $\boldsymbol{B}_{\text{ext}}$ for Fully Kinetic and Hybrid models. Left: Fully kinetic for both electrons and ions (FK). Middle: Drift-kinetic electrons with fully kinetic ions (Hybrid). Right: Drift-kinetic for both electrons and ions (DK).

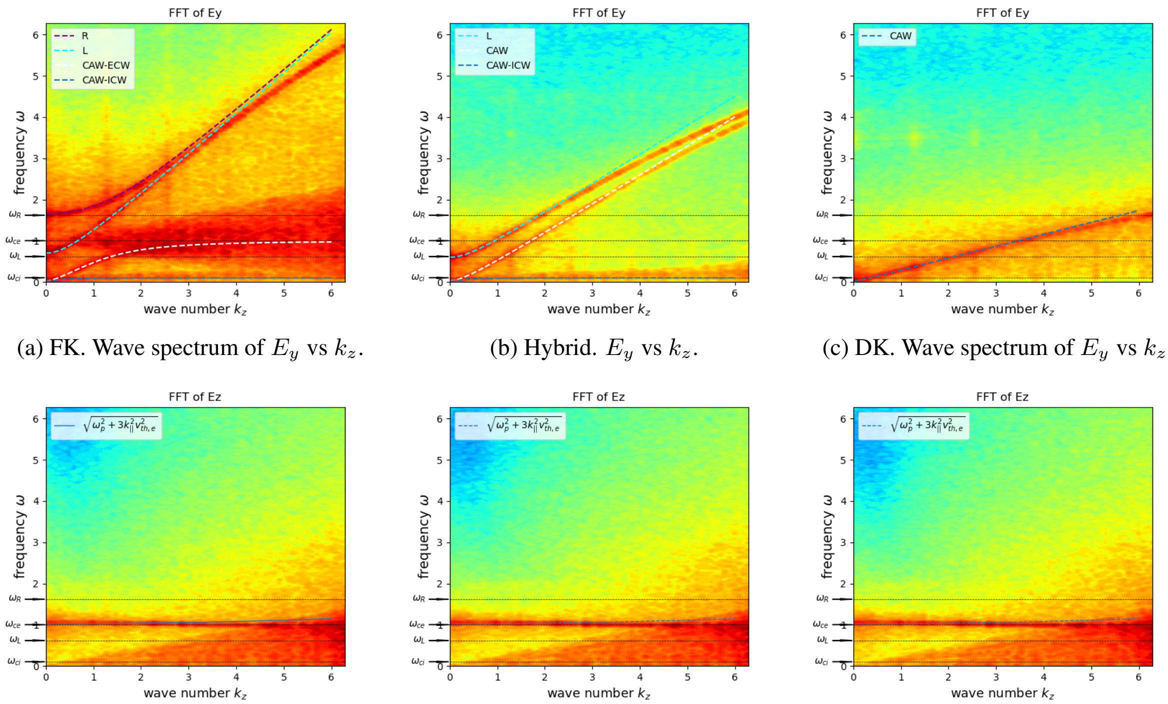

(a) FK. Wave spectrum of E_y vs k_z.

(b) Hybrid. E_y vs k_z.

(c) DK. Wave spectrum of E_y vs k_z.

(d) FK. Wave spectrum of E_z vs k_z.

(e) Hybrid. E_z vs k_z.

(f) DK. Wave spectrum of E_z vs k_z.

FIG. 4. Compare the waves with k parallel to $\boldsymbol{B}_{\text{ext}}$ for the Fully Kinetic and Hybrid models. Left: Fully kinetic for both electrons and ions (FK). Middle: Drift-kinetic electrons with fully kinetic ions (Hybrid). Right: Drift-kinetic for both electrons and ions (DK).

kinetic models, preserving structure and enabling hybrid simulations. Future work will integrate quasi-neutrality assumptions to suppress light waves and address Darwin approximations, further optimizing for edge plasma studies.

ACKNOWLEDGEMENTS

The authors would like to thank Dr. Zhixin Lu, Dr. Roman Hatzky for insightful discussions on GK simulations. This work has been carried out within the framework of the EUROfusion Consortium, funded by the European Union via the Euratom Research and Training Programme (Grant Agreement No 101052200 - EUROfusion). Views and opinions expressed are however those of the author(s) only and do not necessarily reflect those of the European Union or the European Commission. Neither the European Union nor the European Commission can be held responsible for them.

REFERENCES

REFERENCES

[1] Guo Meng, Katharina Kormann, Emil Poulsen, and Eric Sonnendrücker. A geometric particle-in-cell discretization of the drift-kinetic and fully kinetic vlasov-maxwell equations. *Plasmas Physics and Controlled Fusion*, 2025 (submitted).

[2] Katharina Kormann and Eric Sonnendrücker. A dual grid geometric electromagnetic particle in cell method. *SIAM Journal on Scientific Computing*, 46(5):B621–B646, 2024.

[3] P. J. Morrison. Hamiltonian description of the ideal fluid. *Rev. Mod. Phys.*, 70:467–521, Apr 1998.

[4] Philip J Morrison. Structure and structure-preserving algorithms for plasma physics. *Physics of Plasmas*, 24(5):055502, 2017.

[5] Michael Kraus, Katharina Kormann, Philip J Morrison, and Eric Sonnendrücker. GEMPIC: geometric electromagnetic particle-in-cell methods. *Journal of Plasma Physics*, 83(4):905830401, 2017.

[6] Yang Chen and Scott E Parker. Particle-in-cell simulation with Vlasov ions and drift kinetic electrons. *Physics of Plasmas*, 16(5), 2009.

[7] L Chen, Y Lin, XY Wang, and J Bao. A new particle simulation scheme using electromagnetic fields. *Plasma Physics and Controlled Fusion*, 61(3):035004, 2019.

[8] MH Rosen, ZX Lu, and Matthias Hoelzl. An E and B gyrokinetic simulation model for kinetic Alfvén waves in tokamak plasmas. *Physics of Plasmas*, 29(2), 2022.

[9] ZX Lu, G Meng, Matthias Hoelzl, and Ph Lauber. The development of an implicit full f method for electromagnetic particle simulations of Alfvén waves and energetic particle physics. *Journal of Computational Physics*, 440:110384, 2021.

[10] Liu Chen, HaoTian Chen, Fulvio Zonca, and Yu Lin. A gyrokinetic simulation model for low frequency electromagnetic fluctuations in magnetized plasmas. *SCIENCE CHINA Physics, Mechanics & Astronomy*, 64(4):245211, 2021.

[11] J. W. Burby and A. J. Brizard. Gauge-free electromagnetic gyrokinetic theory. *Phys. Lett. A*, 383(18):2172–2175, Juni 2019.

[12] John H Williamson. Low-storage Runge–Kutta schemes. *Journal of computational physics*, 35(1):48–56, 1980.

[13] Thomas H Stix. *Waves in plasmas*. Springer Science & Business Media, 1992.

[14] Hua-sheng Xie. Bo: A unified tool for plasma waves and instabilities analysis. *Computer Physics Communications*, 244:343–371, 2019.